

# Probing the molecular determinants of aniline dioxygenase substrate specificity by saturation mutagenesis

Ee L. Ang<sup>1,2</sup>, Jeffrey P. Obbard<sup>3</sup> and Huimin Zhao<sup>1,4,5</sup>

1 Department of Chemical and Biomolecular Engineering, University of Illinois at Urbana-Champaign, Urbana, IL USA

2 Department of Chemical and Biomolecular Engineering, National University of Singapore, Singapore

3 Division of Environmental Science and Engineering, National University of Singapore, Singapore

4 Center for Biophysics and Computational Biology, University of Illinois at Urbana-Champaign, Urbana, IL, USA

5 Department of Chemistry, University of Illinois at Urbana-Champaign, Urbana, IL, USA

## Keywords

aniline dioxygenase; homology modeling; saturation mutagenesis; substrate specificity

## Correspondence

H. Zhao, Department of Chemical and Biomolecular Engineering, University of Illinois at Urbana-Champaign, 600 South Mathews Avenue, Urbana, IL 61801, USA  
Fax: +1 217 333 5052  
Tel: +1 217 333 2631  
E-mail: zhao5@uiuc.edu

(Received 28 October 2006, revised 5 December 2006, accepted 8 December 2006)

doi:10.1111/j.1742-4658.2007.05638.x

Aniline dioxygenase is a multicomponent Rieske nonheme-iron dioxygenase enzyme isolated from *Acinetobacter* sp. strain YAA. Saturation mutagenesis of the substrate-binding pocket residues, which were identified using a homology model of the  $\alpha$  subunit of the terminal dioxygenase (AtdA3), was used to probe the molecular determinants of AtdA substrate specificity. The V205A mutation widened the substrate specificity of aniline dioxygenase to include 2-isopropylaniline, for which the wild-type enzyme has no activity. The V205A mutation also made 2-isopropylaniline a better substrate for the enzyme than 2,4-dimethylaniline, a native substrate of the wild-type enzyme. The I248L mutation improved the activity of aniline dioxygenase against aniline and 2,4-dimethylaniline approximately 1.7-fold and 2.1-fold, respectively. Thus, it is shown that the  $\alpha$  subunit of the terminal dioxygenase indeed plays a part in the substrate specificity as well as the activity of aniline dioxygenase. Interestingly, the equivalent residues of V205 and I248 have not been previously reported to influence the substrate specificity of other Rieske dioxygenases. These results should facilitate future engineering of the enzyme for bioremediation and industrial applications.

Aniline and its derivatives are widely used as intermediates in the pharmaceutical and azo-dye-manufacturing industries [1,2], and may be released to the environment through effluent streams from these industries [3]. These compounds are highly toxic, and there have been numerous reports on their carcinogenic effects [4–9]. Biodegradation is the main route for removal of aromatic amine pollutants from the natural environment [10], with hydroxylation of the aromatic ring constituting the first step of biodegradation [11]. Thus, an enzyme with the ability to hydroxy-

late a wide range of aniline homologs would be a practical and valuable biocatalyst for the remediation of harmful aromatic amine contaminants.

Aniline dioxygenase (AtdA) is a multicomponent enzyme isolated from *Acinetobacter* sp. strain YAA, which carries out the simultaneous deamination and oxygenation of aniline and 2-methylaniline (2MA) to produce catechol and 3-methylcatechol, respectively [12,13]. AtdA is encoded by five genes (*atdA1–A5*) that produce four putative components: AtdA1, which is a glutamine synthetase-like protein; AtdA2, which is a

## Abbreviations

AtdA, aniline dioxygenase from *Acinetobacter* sp. strain YAA; 24DMA, 2,4-dimethylaniline; 34DMA, 3,4-dimethylaniline; 2EA, 2-ethylaniline; IPTG, isopropyl thio- $\beta$ -D-galactoside; 2IPA, 2-isopropylaniline; 3IPC, 3-isopropylcatechol; 2MA, 2-methylaniline; NDO, naphthalene dioxygenase from *Pseudomonas* sp. strain NCIB 9816-4; 1NDO, crystal structure of naphthalene dioxygenase from *Pseudomonas* sp. strain NCIB 9816-4; 2SBA, 2-*sec*-butylaniline; 2TBA, 2-*tert*-butylaniline; 1ULJ, crystal structure of biphenyl dioxygenase from *Rhodococcus* sp. strain RHA1; 1WQL, crystal structure of cumene dioxygenase from *Pseudomonas fluorescens* IP01.

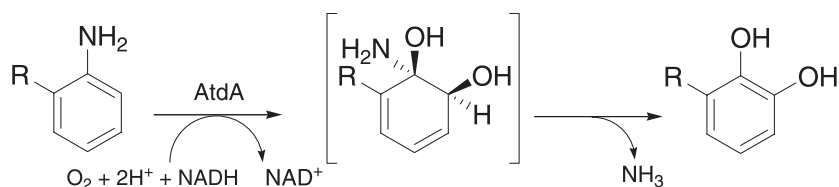


**Fig. 1.** Putative aniline dioxygenation pathway of AtdA. Oxygen atoms are incorporated by AtdA into the 1 and 2 positions of the aniline aromatic ring to form a diol, and the amino group then leaves the ring spontaneously, or with the aid of AtdA1 and AtdA2, as suggested by Takeo *et al.* 1998 [12].

glutamine amidotransferase-like protein; AtdA3 and AtdA4, which resemble the large ( $\alpha$ ) and small ( $\beta$ ) subunits of the terminal class dioxygenase, respectively; and AtdA5, which is a reductase component [12]. The putative reaction pathway of the AtdA enzyme is shown in Fig. 1. It should be noted that the role of each component is speculative, as there has been no detailed characterization of the function of each component in AtdA, or other closely related aniline dioxygenases, such as that from *Pseudomonas putida* UCC22 (pTDN1) [14]. The lack of characterization of the structural determinant of the substrate specificity of the AtdA enzyme has thus limited its development as a biocatalyst for the bioremediation of a wide range of aromatic amines.

It has been reported that the substrate specificities of various dioxygenases, such as the naphthalene, biphenyl and 2,4-dinitrotoluene dioxygenases, are determined by their terminal  $\alpha$  subunits [15–17]. Mutational studies have been carried out on biphenyl dioxygenase [18] and naphthalene dioxygenase [19,20]. On the basis of these findings, various directed evolution and saturation mutagenesis studies on the terminal  $\alpha$  subunits have been performed; these have successfully altered the substrate specificity of these dioxygenases [21–26]. These results and the findings of the gene deletion assay in this work indicate the likelihood that AtdA3 controls the substrate specificity of AtdA. However, unlike the dioxygenases in the above-mentioned studies, which only require the  $\alpha$  and  $\beta$  terminal dioxygenase subunits as well as the reductase component to carry out the benzene ring hydroxylation reactions, AtdA has been reported to require all four components to display aniline-hydroxylating activity [27]. To date, it has not been reported which of the five genes control the substrate specificity of the AtdA enzyme.

The objective of this study was to identify and probe the residues determining the activity as well as the substrate specificity of AtdA, using molecular modeling and saturation mutagenesis of the substrate-binding pocket residues in AtdA3. The structure–function

relationship elucidated from this work can potentially be applied to the further engineering of AtdA to widen its utility as a biocatalyst. A homology model was built using the crystal structures of naphthalene dioxygenase from *Pseudomonas* sp. strain NCIB 9816-4 (1NDO) [28], biphenyl dioxygenase from *Rhodococcus* sp. strain RHA1 (1ULJ) [29] and cumene dioxygenase from *Pseudomonas fluorescens* IP01 (1WQL) [30] as templates. Fourteen residues within 4.5 Å of the substrate, forming the substrate-binding pocket, were selected for saturation mutagenesis studies. Saturation mutagenesis of the substrate-binding pocket residues widened the substrate specificity of AtdA to include 2-isopropylaniline (2IPA), for which the wild-type (WT) enzyme has no activity. The activities of AtdA with aniline and 2,4-dimethylaniline (24DMA) as substrate were also improved 1.7-fold and 2.1-fold, respectively.

This is the first study on the molecular determinants of the substrate specificity of a four-component dioxygenase, AtdA, and it has shown that the  $\alpha$  subunit of the terminal dioxygenase (AtdA3) indeed plays a role in the substrate specificity of AtdA. Results from this work will have important implications for the engineering of aniline dioxygenases for the deamination of aromatic amines, bioremediation, and other industrial applications.

## Results

### Substrate specificity of AtdA

As the substrate range of AtdA had not been extensively characterized, it was necessary to determine this property before probing the molecular determinants of the enzyme's substrate specificity. To determine the substrate specificity of the WT AtdA, *Escherichia coli* JM109 expressing the WT enzyme was incubated individually with a series of *ortho*-substituted anilines with progressively larger alkyl side chains, namely, aniline, 2MA, 2-ethylaniline (2EA), 2IPA, 2-*sec*-butylaniline (2SBA), and 2-*tert*-butylaniline (2TBA), as well as two xylidine substrates, 24DMA and 3,4-dimethylaniline

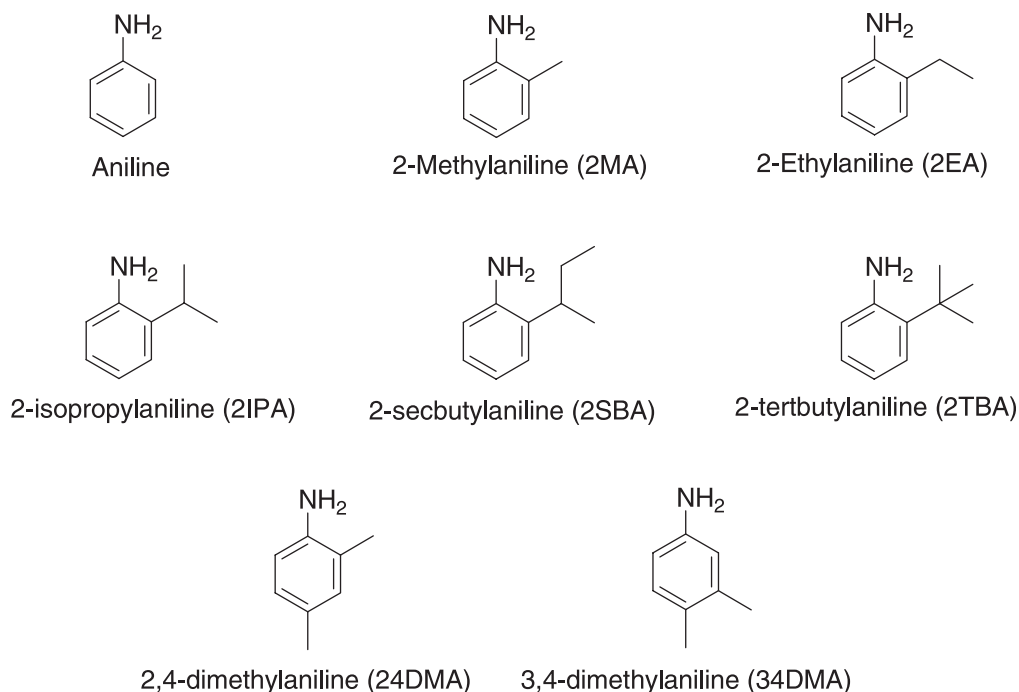


**Fig. 2.** *Ortho*-substituted aniline and xylylene substrates used to determine the substrate specificity of AtdA.

(34DMA), as shown in Fig. 2. Dihydroxylation of a particular substrate by the enzyme produces its corresponding catechol, which undergoes auto-oxidation to form colored compounds, indicating activity against that substrate [22,27,31,32].

Among the *ortho*-substituted substrates, the WT AtdA showed activity for aniline, 2MA, and 2EA. However, the enzyme was inactive against substrates with an *ortho* side chain larger than an ethyl group (2IPA, 2SBA and 2TBA). As 2EA and 2IPA differ only by a single methyl group on the *ortho* side chain, the substrate specificity of the enzyme is most probably controlled by steric hindrance of the *ortho* side chain along the substrate channel or in the substrate-binding pocket. Among the xylylene substrates, 24DMA was accepted as a substrate, but the change of the position of a methyl group from *ortho* (24DMA) to *meta* (34DMA) rendered the substrate unacceptable to the enzyme. This may indicate that the steric limitation of the enzyme's binding pocket takes place in the area between the *ortho* and *para* positions of the aromatic substrate.

On the basis of these results, aniline and 24DMA were chosen as target substrates to probe for residues determining the activity of AtdA3, whereas 2IPA and 2SBA were chosen as target substrates to probe for residues controlling the substrate specificity of the enzyme.

### Gene deletion assay

To narrow the range of candidates for saturation mutagenesis studies, a gene deletion assay was carried out to identify the subunit(s) critical for AtdA activity. The *atdA1*, *atdA2* and *atdA3* genes were targeted in this assay. The AtdA4 subunit, which is homologous to the  $\beta$  subunit of a terminal Rieske dioxygenase, was not targeted because the  $\alpha$  subunit of the Rieske dioxygenase is generally regarded as the main contributor to substrate specificity [17,33,34]. The *atdA5* gene encodes a reductase that is involved in cofactor regeneration in the dihydroxylation reaction, and not in the direct binding of the substrate. Hence, it was not targeted in the gene deletion assay.

The *atdA* genes were first cloned into expression vectors as described in Experimental procedures. *E. coli* BL21(DE3) cells harboring the various plasmid combinations described in Table 1 were then tested for activity against 2MA. In the absence of the *atdA1* or *atdA3* gene, no activity against 2MA was detected. On the other hand, 2MA activity was detected in an *E. coli* BL21(DE3) cell line in which *atdA2* was deleted (Table 1). Hence, AtdA1 and AtdA3 are critical for the activity of the enzyme and provide good starting points for the study of the molecular determinants of the substrate specificity and activity of AtdA.

**Table 1.** Results of the gene deletion assay, together with the plasmids used for each gene deletion construct.

Gene deleted	Plasmids transformed into <i>E. coli</i> BL21(DE3)	Activity against 2MA
<i>atdA1</i>	pACYC A2 and pET A3A4A5	–
<i>atdA2</i>	pACYC A1 and pET A3A4A5	+
<i>atdA3</i>	pACYC A1A2 and pET A4A5	–
Control (no deletion)	pACYC A1A2 and pET A3A4A5	+

On the basis of the results of this assay and mutational studies on the  $\alpha$  subunits of other dioxygenases [18–26], the AtdA3 subunit was first targeted for saturation mutagenesis studies to probe for the molecular determinants of the enzyme's substrate specificity and activity. It should be noted that this assay was intended to aid in determining which AtdA subunit would be studied first, and the possibility that the other subunits may play a part in substrate specificity and activity should not be ruled out. In order to study the AtdA3 subunit, we started from residues in direct contact with the substrate – the substrate-binding pocket residues.

### Identification of substrate-binding pocket residues

To identify the substrate-binding pocket of AtdA3, the largest substrate accepted by the WT AtdA, 2EA, was docked into the AtdA3 homology model. The approximate initial position of the substrate was determined on the basis of the possible binding sites identified by the Site Finder function in MOE, as well as the relative position of the indole substrate in the crystal structure of naphthalene dioxygenase from *Pseudomonas* sp. strain NCIB 9816-4 (NDO) (Protein Data Bank accession code 1O7N). Eighteen residues within the van der Waals contact distance (4.5 Å) of the substrate were identified as substrate-binding pocket residues (Fig. 3A). These residues are N198, D201, G202, H204, V205, H209, L213, I248, Q250, K256, E257, W260, A293, G294, N296, L304, F348, and D356.

### Saturation mutagenesis

From the sequence alignment of AtdA3 with NDO [35], biphenyl dioxygenase [29], and cumene dioxygenase [30], residues H204, H209 and D356 correspond to the catalytic facial triad that coordinates the mononuclear iron in the active site (H208, H213 and D362 of NDO), whereas D201 corresponds to D205 of NDO, which plays a critical role in electron transfer between the Rieske [2Fe–2S] center of one  $\alpha$  subunit

and mononuclear iron in the adjacent  $\alpha$  subunit [36]. Hence, these four critical residues were not subjected to saturation mutagenesis. The remaining 14 sites were mutagenized individually using the NNS codon (where N denotes A, T, G or C, and S denotes G or C), resulting in 32 possible codon combinations for each site encoding all possible 20 amino acids. One hundred and eighty-six clones were screened in two 96-well microplates per site, ensuring comprehensive coverage of all possible 19 mutations at each site, with three WT clones as control in each plate. Random clones were sequenced to ensure that the corresponding codons were successfully randomized, and none had the parental sequence.

Each library was screened using the Gibbs' reagent screening method adapted from Sakamoto *et al.* [26], with modifications as elaborated in Experimental procedures. Mutants were selected on the basis of improved activity against compounds that are substrates of the WT enzyme (aniline and 24DMA), or novel activity against the substrates 2IPA and 2SBA.

From the V205 saturation mutagenesis library, several mutants with novel activity against 2IPA, a substrate not accepted by the WT enzyme, were found. DNA sequencing of these mutants revealed that all had the V205A mutation. The mutagenesis library of I248 yielded two mutants with improved aniline and 24DMA activity. Both mutants had the I248L mutation.

In studies on various other dioxygenases, the mutagenesis of the residue corresponding to F348 of AtdA3 (F352 of NDO) significantly altered the activity or the substrate specificity of the dioxygenase [19,20,24,37–39]. However, mutation of residue F348 critically impaired the activity of the enzyme in this case. From the saturation mutagenesis library of residue 348, only five active mutants were found, three of which had the parent residue, phenylalanine, at position 348. These residues were encoded by codon TTC instead of the parental codon TTT. The other two active mutants were valine and tryptophan mutants, neither of which had improved activity against aniline or 24DMA, or novel activity against 2IPA or 2SBA.

### SDS/PAGE analysis

Expression levels of AtdA in the V205A and I248L mutants were compared to that of the WT enzyme using SDS/PAGE. Visual inspection of the SDS/PAGE gel showed no observable difference between the concentrations of the AtdA1 (56.8 kDa), AtdA2 (28.5), AtdA3 (50.3 kDa), AtdA4 (24.0 kDa) and AtdA5 (37.2 kDa) subunits in the mutants as compared to their

**Table 2.** Conversion rate of 2-isopropylalnine (2IPA), aniline and 2,4-dimethylalanine (24DMA) by *E. coli* JM109 expressing the wild-type AtdA enzyme and the V205A and I248L mutants.

AtdA3	2IPA		Aniline		24DMA	
	Rate (nmol·min <sup>-1</sup> ·mg <sup>-1</sup> protein)	Relative rate	Rate (nmol·min <sup>-1</sup> ·mg <sup>-1</sup> protein)	Relative rate	Rate (nmol·min <sup>-1</sup> ·mg <sup>-1</sup> protein)	Relative rate
WT	0	–	26.0 ± 0.20	1.00	2.8 ± 0.1	1.00
V205A	1.1 ± 0.2	∞	3.1 ± 0.10	0.12	0.1 ± 0.02	0.03
I248L	0	–	45.3 ± 7.20	1.74	5.9 ± 0.01	2.10

corresponding subunits in the WT enzyme (supplementary Fig. S1). Thus, the changes in activity and specificity of the mutants did not result from altered expression.

### Whole-cell activity against 2IPA

The positive mutants of each library were characterized using the whole-cell activity assay as described in Experimental procedures. The V205A mutation introduced a novel activity to the AtdA enzyme, enabling *E. coli* whole cells expressing the mutant to convert 2IPA at a rate of 1.1 nmol·min<sup>-1</sup>·mg<sup>-1</sup> protein to form 3-isopropylcatechol (3IPC) as the only product (Table 2). The identity of 3IPC was confirmed by comparing its HPLC retention time with that of the authentic standard, as well as by coelution with the authentic standard, and LC-MS analysis ( $m/z = 151$ ). In contrast, the 2IPA-dihydroxylation activity was not detected at all in the WT enzyme or the I248L mutant. The V205A mutation also made the enzyme a better catalyst for the conversion of 2IPA, a substrate not accepted by the WT enzyme, than for 24DMA, a substrate accepted by the WT enzyme.

### Whole-cell activity against aniline and 24DMA

The rate of catechol formation from aniline by whole cells expressing the I248L mutant was 45.3 nmol·min<sup>-1</sup>·mg<sup>-1</sup> protein, a 1.7-fold enhancement over the WT enzyme, whereas that of the V205A mutant was reduced to 3.1 nmol·min<sup>-1</sup>·mg<sup>-1</sup> protein (Table 2). For both these mutants, as well as the WT enzyme, the only product formed was catechol, as confirmed by HPLC coelution with the authentic catechol standard and LC-MS analysis ( $m/z = 109$ ).

The 24DMA conversion rate of the I248L mutant was enhanced 2.1-fold over that of the WT enzyme, to 5.9 nmol·min<sup>-1</sup>·mg<sup>-1</sup> protein. On the other hand, the 24DMA activity of the V205A mutant was reduced to 0.1 nmol·min<sup>-1</sup>·mg<sup>-1</sup> protein (Table 2). The 24DMA conversion products from the I248L,

V205A and WT enzymes had the same HPLC elution time, and all had a molecular ion at  $m/z = 137$ , corresponding to that of a dimethylcatechol, when analyzed with LC-MS. However, as there was no authentic standard, the product of 24DMA conversion by the WT enzyme was purified and further analyzed using <sup>1</sup>H-NMR. The two methyl groups were detected at  $\delta$  2.20 (s) and  $\delta$  2.21 (s), the two aromatic protons at  $\delta$  7.26 (s), and the two hydroxyl groups at  $\delta$  6.51 (s) and  $\delta$  6.54 (s), confirming the product to be 3,5-dimethylcatechol. Thus, the regioselectivity of the enzyme was not altered by the I248L or V205A mutations, as the only product from 24DMA conversion was 3,5-dimethylcatechol.

### Discussion

This is the first study on the molecular determinants for substrate specificity of a four-component Rieske dioxygenase, AtdA. In this study, we constructed a homology model to identify the residues defining the substrate-binding pocket of the  $\alpha$  subunit, AtdA3, and applied saturation mutagenesis to these residues to probe the molecular determinants of the activity and specificity of the enzyme. We have clearly shown that the substrate specificity of AtdA can indeed be controlled by the AtdA3 subunit. The V205A mutation enables the enzyme to dihydroxylate 2IPA, a substrate not accepted by the WT enzyme, and the I248L mutation enhances the activity of the enzyme against aniline and 24DMA, a carcinogenic pollutant for which no enzyme directly responsible for its biodegradation has been identified to date.

Interestingly, residues V205 and I248 have not been previously reported to influence the substrate specificity of a Rieske dioxygenase. The V205 residue corresponds to V209 in NDO [35], V207 of naphthalene dioxygenase from *Ralstonia* sp. strain U2 (NagAc) [40], A223 of toluene-2,3-dioxygenase (TodC1) [41], and A234 of biphenyl dioxygenases from *Burkholderia xenovorans* LB400 and *P. pseudoalcaligenes* KF707 [42,43].

On the basis of the homology model of AtdA3, residue V205 resides in the deepest and narrowest end of the substrate-binding pocket, and is found next to the facial triad of H204, H209 and D356, which coordinates the catalytic mononuclear iron. From the docking of 2IPA into the V205A mutant binding pocket, it was found that the isopropyl side chain of 2IPA comes within 4.25 Å of the A205 side chain (Fig. 3B). In contrast, if 2IPA were to assume this position in the binding pocket of the WT enzyme, the side chain of V205 would come within 2.74 Å of the isopropyl side chain of 2IPA (Fig. 3C). This could result in a steric clash that forces the substrate away from the active site iron,

and prevents the substrate from coming into contact with the activated oxygen molecule bound to the catalytic iron, possibly explaining the lack of activity of the WT enzyme against 2IPA. Removal of the methyl groups from residue 205 via a valine to alanine mutation removes the steric hindrance and allows the approach of 2IPA towards the catalytic iron.

Residue I248 lies at the entrance of the substrate-binding pocket of the enzyme, leading to the substrate channel. Mutation from isoleucine to leucine results in a larger entrance to the substrate-binding pocket (Fig. 3D,E). This may allow for easier entry and exit of substrate and product molecules, explaining the

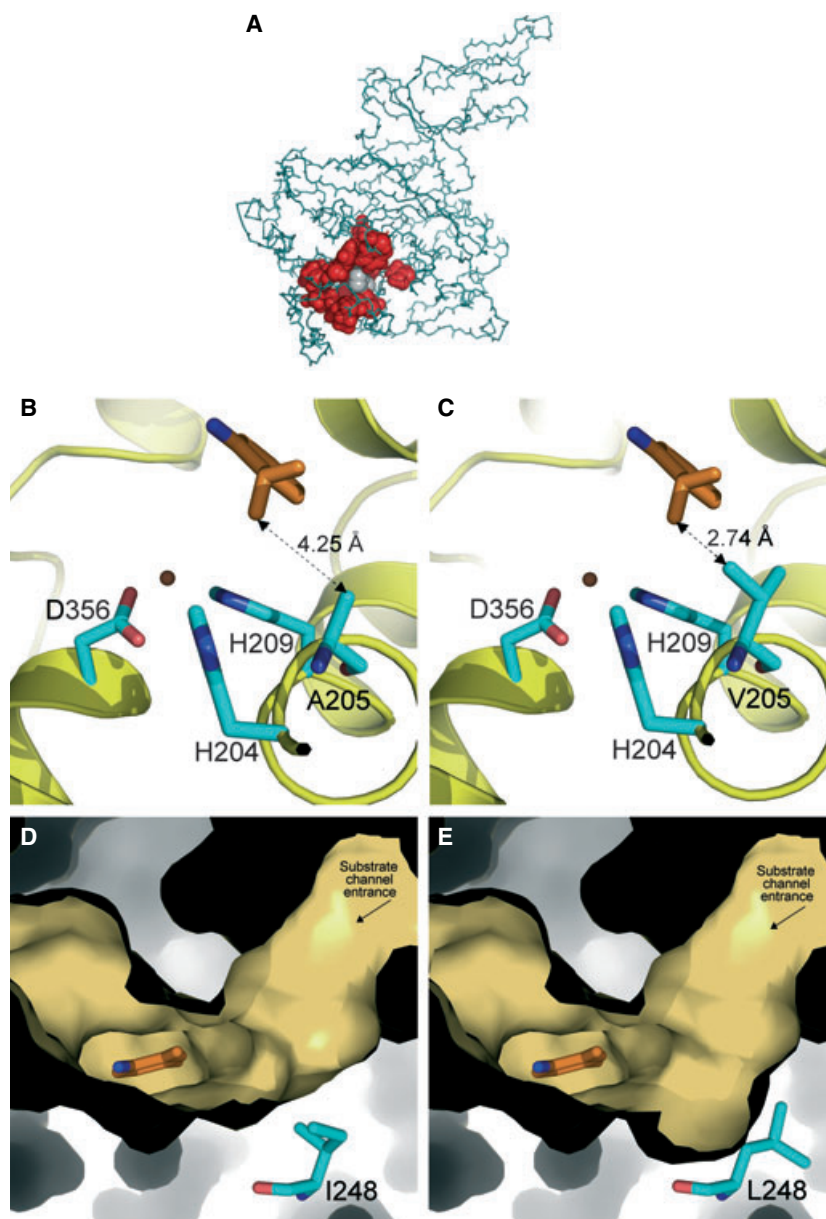


**Fig. 3.** (A) The homology model of the AtdA3, with the substrate binding pocket residues highlighted in red and the docked substrate 2EA in gray. (B,C) The position of the substrate, 2IPA, relative to residue 205 in the substrate binding pocket of the V205A mutant (B) and WT AtdA3 (C). Also shown are the mononuclear iron (brown sphere) and the catalytic facial triad of H204, H209 and D356. (D,E) Molecular surfaces of the substrate channel leading to the binding pocket of the WT AtdA3 (D) and the mutant I248L (E). The substrate positions are simulated using the docking function in the MOE software. Figures were generated using the PYMOL software (De Lano Scientific LLC, South San Francisco, CA).

increase in activity of the enzyme for all the substrates screened.

Although it has been shown in this work that AtdA3 controls the substrate specificity of AtdA, we have yet to explore the AtdA1 and AtdA2 components. AtdA1 has 25.8% homology to glutamine synthetases from *Salmonella typhimurium* [44], and the important ATP-binding motif and the tyrosine 426 corresponding to the adenylation site in glutamine synthetases are well conserved. AtdA1 also has 62.1% protein sequence identity with TdnQ of the aniline dioxygenase from *P. putida* UCC22. It was reported that *E. coli* cells expressing TdnQ had no glutamine synthetase activity [14], suggesting that AtdA1 is unlikely to be involved in the recovery of nitrogen for biosynthesis reactions. AtdA2 exhibits homology to the class I glutamine amidotransferase domain in GMP synthetase [45]. It has been postulated that, as glutamine synthetase and glutamine amidotransferase are involved in the addition of an amino group to glutamate and its release from glutamine, respectively, AtdA1 and AtdA2 may be involved in the recognition and release of aniline amino groups [12]. Hence, a similar engineering approach with AtdA1 and AtdA2 may offer useful insights into the substrate specificity and activity of the enzyme.

In summary, we have shown, by saturation mutagenesis of the subunit's substrate-binding pocket residues, that the substrate specificity as well as the activity of the four-component Rieske dioxygenase, AtdA, can be controlled by the  $\alpha$  subunit of the terminal dioxygenase, AtdA3. We found that the V205A mutation had the greatest effect on the substrate specificity of the enzyme, as the mutant was able to dihydroxylate 2IPA, a substrate previously not accepted by the WT enzyme, whereas residue I248 plays a role in the activity of the enzyme. Although the V205A mutation caused the loss of activity against aniline and 24DMA, the primary goal of this work, which was to probe the molecular determinants of AtdA, was achieved. This finding should facilitate future engineering of the enzyme for bioremediation and industrial applications, using methods such as random mutagenesis or DNA shuffling.

## Experimental procedures

### Materials

Aniline, 24DMA, 34DMA, 2MA, 2EA, 2IPA, 2SBA, 2TBA, catechol, isopropyl- $\beta$ -D-thiogalactoside (IPTG), dimethylformamide, ampicillin and all other chemicals were purchased from Sigma (St Louis, MO) unless otherwise

stated. 3IPC was purchased from Chem Service (West Chester, PA). Gibbs' reagent was purchased from MP Bio-medicals (Solon, OH). The Quikchange XL Site Directed Mutagenesis kit and *Pfu* Turbo DNA polymerase were purchased from Stratagene (La Jolla, CA). Primers were purchased from Integrated DNA Technologies (Coralville, IA) and 1st Base (Singapore). PCR-grade deoxynucleotide triphosphates (dNTP) were obtained from Roche Applied Sciences (Indianapolis, IN). All DNA-modifying enzymes were purchased from New England Biolabs (Beverly, MA). All DNA gel purifications were carried out using the QIAEX II gel purification kit from Qiagen (Valencia, CA). All plasmid isolations were performed using the QIAprep Miniprep kit from Qiagen.

*Escherichia coli* JM109 and BL21(DE3) were purchased from Novagen (Madison, WI), and chemically competent *E. coli* DH5 $\alpha$  was purchased from the Cell Media Facility at the University of Illinois (Urbana, IL). The pTrc99A plasmid was obtained from Amersham Pharmacia (Piscataway, NJ). The pACYCDuet-1 and pETDuet-1 plasmids were obtained from Novagen. The pAS91 and pAS93 plasmids, both containing the AtdA gene cluster, were kindly provided by M Takeo from the Department of Applied Chemistry, Himeiji Institute of Technology, Hyogo, Japan.

### Plasmid construction

The sequences of all primers used in the construction of plasmids are given in supplementary Table S1. From plasmid pAS91, the gene segment containing *atdA1A2* was amplified using primers pTrcA1 F and pTrcA2 RII, the *atdA3* gene was amplified using primers pTrcA3 FII and pTrcA3 RII, and the gene segment containing *atdA4A5* was amplified using primers pTrcA4 FII and pTrcA5 RII. The PCR products were gel purified using a QIAEX II gel purification kit, and treated with the restriction enzyme *DpnI* to remove any residual methylated template from the products. Overlap extension PCR was used to join the three fragments together. The overlap extension PCR reaction mix consisted of 85 ng of *atdA1A2*, 50 ng of *atdA3*, 60 ng of *atdA4A5*, 2  $\mu$ L of 10 $\times$  *Pfu* buffer, 2  $\mu$ L of 10 $\times$  dNTP (mixture of dATP, dTTP, dGTP, and dCTP, each at a concentration of 100 mM), 2 U of *Pfu* Turbo DNA polymerase, and water to a final volume of 20  $\mu$ L. The PCR program consisted of 94  $^{\circ}$ C for 2 min, 10 cycles of 94  $^{\circ}$ C for 1 min, 55  $^{\circ}$ C for 1.5 min, and 72  $^{\circ}$ C for 6 min, and a final extension for 10 min at 72  $^{\circ}$ C. The reconstituted *atdA* operon was gel purified, digested with *SalI* restriction enzyme, and ligated into pTrc99A using T4 DNA ligase. Subsequently, the *EcoRI* restriction site on *atdA2* was removed by introducing silent mutations to the GAATTC recognition site (521–526 bp), changing it to GTATCC. The Quikchange XL Site Directed Mutagenesis kit was used for introduction of this mutation, according to the PCR and transformation protocol recommended in the

manual. The resulting plasmid, pTA2-3, was used for all assays in this work except the gene deletion studies.

To construct the plasmids for the gene deletion assay, the *atdA1* gene was amplified using the A1\_EcoRI\_F and A1\_SalI\_R primers. The *atdA2* gene was amplified using the A2\_FseI\_F and A2\_AvrII\_R primers. The *atdA3* gene was amplified using the A3\_EcoRI\_F and A3\_SalI\_R primers. The *atdA4A5* gene was amplified using the A4\_FseI\_F and A5\_AvrII\_R primers. The PCR reaction mix for each gene consisted of 150 ng of the pTA2-3 template, 50 pmol each of the forward and reverse primers, 10  $\mu$ L of 10 $\times$  *Taq* polymerase buffer, 6  $\mu$ L of 25 mM MgCl<sub>2</sub>, 10  $\mu$ L of 10 $\times$  dNTP, 1.25 U each of *Taq* DNA polymerase and *Pfu* Turbo DNA polymerase, and water to a final volume of 100  $\mu$ L. The PCR program consisted of 94 °C for 3 min, 25 cycles of 94 °C for 45 s, 50 °C for 45 s, and 72 °C for 2 min, and a final extension of 7 min at 72 °C. The PCR products were then gel purified. The *atdA1* and *atdA3* PCR products were digested with *EcoRI* and *SalI*, and the *atdA2* and *atdA4A5* PCR products were digested with *FseI* and *AvrII*.

To construct plasmid pACYC A1, the pACYCDuet-1 plasmid was digested with *EcoRI* and *SalI*, gel purified, and ligated with the digested *atdA1* PCR product. To construct pACYC A2, the pACYCDuet-1 plasmid was digested with *FseI* and *AvrII*, gel purified, and ligated with the digested *atdA2* PCR product. To construct pACYC A1A2, the pACYC A2 plasmid was digested with *EcoRI* and *SalI*, gel purified, and ligated with the digested *atdA1* PCR product. To construct plasmid pET A4A5, the pETDuet-1 plasmid was digested with *FseI* and *AvrII*, gel purified, and ligated with the digested *atdA4A5* PCR product. To construct plasmid pET A3A4A5, the pETA4A5 plasmid was digested with *EcoI* and *SalI*, gel purified, and ligated with the digested *atdA3* PCR product. All ligations were carried out overnight at 16 °C using the T4 DNA ligase. The salts from the ligation reactions were then removed by precipitating the ligated DNA with n-butanol [46]. The ligation products were then transformed into *E. coli* BL21(DE3) by electroporation. The various plasmids were then rescued and retransformed into *E. coli* BL21(DE3) according to Table 1.

### Substrate specificity assay

*Escherichia coli* JM109 cells expressing AtdA were inoculated into 5 mL of LB medium with ampicillin (100 mg·L<sup>-1</sup>) and grown overnight in a 37 °C shaker at 250 r.p.m. Subsequently, 0.3 mL of the overnight culture was inoculated into 3 mL of M9 minimal medium [47] with 100 mg·L<sup>-1</sup> ampicillin and 1 mM IPTG, and incubated in a 30 °C shaker for 4 h at 250 r.p.m. to induce protein expression. Aniline or its analog substrates were then added to each tube to a final concentration of 1 mM, and the culture was incubated for 1 day in a 30 °C shaker at 250 r.p.m. The culture was then observed for formation of colored oxidation products of catechols.

### Gene deletion assay

*Escherichia coli* BL21(DE3) colonies harboring the various gene deletion constructs were picked into separate culture tubes with 3 mL of LB medium containing 100 mg·L<sup>-1</sup> ampicillin and 35 mg·L<sup>-1</sup> chloramphenicol, and were grown overnight in a 37 °C shaker at 250 r.p.m. Fifty microliters of each of the overnight cultures was inoculated into 5 mL of LB medium with the same antibiotic composition and grown in a 37 °C shaker at 250 r.p.m. At an optical density (*A*<sub>600</sub>) of ~0.5–0.6, IPTG was added to each culture to a final concentration of 1 mM, and the cultures were then incubated for 3 h in a 30 °C shaker at 250 r.p.m.

The cultures were harvested by centrifugation at 6000 *g* for 10 min using the Hettich Universal 32R centrifuge with a 1620A rotor (Tuttlingen, Germany). The supernatant was discarded, and the cell pellets were gently resuspended with 5 mL of M9 minimal medium with 100 mg·L<sup>-1</sup> ampicillin, 35 mg·L<sup>-1</sup> chloramphenicol and 1 mM IPTG. 2MA was then added to each culture to a final concentration of 2 mM, and the cultures were incubated in a 30 °C shaker at 250 r.p.m. for 24 h. The cultures were constantly monitored for the formation of auto-oxidation products.

### Homology modeling

A homology model of AtdA3 was constructed using INSIGHT II software (INSIGHT II, version 2000; Accelrys Inc., San Diego, CA). The crystal structures of naphthalene dioxygenase (1NDO) [28], biphenyl dioxygenase (1ULJ) [29], and cumene dioxygenase (1WQL) [30] were used as templates. The sequence of AtdA3 was aligned with those of 1NDO, 1ULJ and 1WQL using CLUSTALW (<http://workbench.sdsc.edu/>), and was adjusted to ensure that critical residues, such as the catalytic iron coordinating the facial triad of AtdA3 (H204, H209, and D356), were aligned with critical residues of NDO (H208, H213, and D362). Gaps in regions of secondary structures were avoided when the sequences were aligned. Three loop optimization models were generated for each model constructed with INSIGHT II. All the models were checked with the Prostat and Profiles-3D functions in INSIGHT II. The model with the highest overall score was chosen. The substrates were docked in the homology models of the WT AtdA3 and the mutants V205A and I248L, using MOE software (Chemical Computing Group Inc., Montreal, Canada). Mutations were introduced into the AtdA3 model using the Rotamer Explorer function, and the rotamer with the lowest free energy was chosen. Each docking run consisted of 25 independent docks with six iteration cycles, and a random start was used to generate substrate positions within the docking box. From the results, the substrate orientation that gave the lowest

interaction energy was chosen for another round of docking. A nonrandom start was used in this case. This process was repeated two times or until there was no significant decrease in the interaction energy of the substrate. The Connolly surface of the substrate-binding pocket was generated using the Molecular Surface function in MOE.

### Saturation mutagenesis

A saturation mutagenesis library at each binding pocket residue was created using the Quikchange XL Site Directed Mutagenesis kit, with plasmid pTA2-3 as the template. The primers listed in supplementary Table S2, together with their complements, were used in the saturation mutagenesis PCR. The PCR and transformation protocol recommended in the manual were used. Transformants were plated on LB agar plates containing  $100 \text{ mg}\cdot\text{L}^{-1}$  ampicillin and incubated overnight in  $37^\circ\text{C}$ .

### Screening method

The screening method was adapted from Sakamoto *et al.* [26], with modifications. Each colony of a library was picked into  $200 \mu\text{L}$  of LB medium containing ampicillin ( $100 \text{ mg}\cdot\text{L}^{-1}$ ) in separate wells of a 96-well microplate. One hundred and eighty-six clones were picked for each target residue, with three WT clones being included as positive controls in each plate. The plates were incubated overnight at  $37^\circ\text{C}$  with shaking at  $250 \text{ r.p.m.}$  Ten microliters of the overnight culture was inoculated into new wells containing  $90 \mu\text{L}$  of M9 minimal medium supplemented with  $5 \mu\text{M}$   $\text{FeSO}_4$ ,  $100 \text{ mg}\cdot\text{L}^{-1}$  ampicillin and  $1 \text{ mM}$  IPTG. Five replicates of each plate were made. The plates were incubated at  $30^\circ\text{C}$  with shaking at  $250 \text{ r.p.m.}$  for  $4 \text{ h.}$  Then,  $100 \mu\text{L}$  of M9 medium with  $5 \mu\text{M}$   $\text{FeSO}_4$ ,  $100 \text{ mg}\cdot\text{L}^{-1}$  ampicillin,  $1 \text{ mM}$  IPTG and  $2 \text{ mM}$  substrate was added to each well of a plate. A different substrate was added to each plate. The substrates were aniline, 24DMA, 2IPA, 34DMA, and 2SBA. The plates were then incubated at  $30^\circ\text{C}$  with shaking at  $250 \text{ r.p.m.}$  for  $45 \text{ min}$  for aniline and for  $4 \text{ h}$  for the other substrates. The absorbance at  $595 \text{ nm}$  was measured after incubation. For aniline, 2IPA and 2SBA,  $75 \mu\text{L}$  of  $0.2 \text{ M}$  HCl was first added to each well, and then  $10 \mu\text{L}$  of  $0.32\%$  (w/v) Gibbs' reagent in ethanol; the absorbance at  $560 \text{ nm}$  was measured after  $30\text{--}50 \text{ min.}$  For 24DMA,  $10 \mu\text{L}$  of  $0.32\%$  Gibbs' reagent was added directly, and the absorbance at  $620 \text{ nm}$  was measured after  $5 \text{ min.}$  The activity of each mutant, as indicated by the absorbance at  $560 \text{ nm}$  or  $620 \text{ nm}$ , was then normalized to its cell density ( $D_{595}$ ). Positive mutants from each screen were subjected to a second screen carried out in larger volumes, using culture tubes instead of 96-well microplates.

### Whole-cell activity assay

An overnight LB culture of JM109 with WT or mutant plasmid was inoculated into  $150 \text{ mL}$  of LB medium to an  $D_{600}$  of  $0.02$ , and incubated in a  $37^\circ\text{C}$  shaker at  $250 \text{ r.p.m.}$  When the  $D_{600}$  reached  $0.50\text{--}0.55$ , IPTG was added to a final concentration of  $1 \text{ mM.}$  The culture was then incubated in a  $30^\circ\text{C}$  shaker at  $250 \text{ r.p.m.}$  for  $3 \text{ h.}$  The induced culture was then centrifuged at  $4000 \text{ g}$  for  $10 \text{ min}$  using the Beckman J2-21M centrifuge with a JA14 rotor (Fullerton, CA). The supernatant was discarded, and the cell pellet was resuspended in  $150 \text{ mL}$  of modified M9 buffer (M9 minimal medium with  $0.1\%$  glucose). The resuspended cells were centrifuged using the same conditions. The supernatant was discarded, and the cell pellet was resuspended in modified M9 buffer to a final  $D_{600}$  of about  $10$ . Then,  $5 \text{ mL}$  of the resuspended cells was aliquoted into a  $50 \text{ mL}$  centrifuge tube, and  $5 \mu\text{L}$  of  $1 \text{ M}$  substrate dissolved in dimethylformamide was added to a final concentration of  $1 \text{ mM.}$  The cells were then incubated at  $30^\circ\text{C}$  with shaking at  $250 \text{ r.p.m.}$  Samples ( $0.5 \text{ mL}$ ) were taken at various time points. The samples were centrifuged at  $16\,000 \text{ g}$  in a benchtop centrifuge (Denville Scientific 260D, Metuchen, NJ) for  $3 \text{ min}$ , and the supernatant was stored at  $-20^\circ\text{C}$  until ready for analysis.

The substrate and products were separated and quantified using HPLC with a  $250 \times 4.60 \text{ mm}$  Synergi  $4 \mu$  Polar-RP 80 A column from Phenomenex (Torrance, CA). All HPLC methods used were isocratic, with a flow rate of  $1 \text{ mL}\cdot\text{min}^{-1}$ . Aniline was analyzed using  $90\%$  potassium phosphate ( $\text{pH } 7.0$ ) and  $10\%$  acetonitrile as mobile phase. 2IPA was analyzed using  $60\%$  potassium phosphate ( $\text{pH } 7.0$ ) and  $40\%$  acetonitrile as mobile phase. 24DMA was analyzed using  $70\%$  potassium phosphate ( $\text{pH } 7.0$ ) and  $30\%$  acetonitrile as mobile phase.

For each culture,  $1 \text{ mL}$  of the resuspended cells was centrifuged at  $6000 \text{ g}$  in a benchtop centrifuge (Denville Scientific 260D) for  $3 \text{ min}$ , and the supernatant was discarded. The cell pellet was resuspended in  $50 \text{ mM}$  Tris/HCl ( $\text{pH } 7.5$ ), and disrupted by a single pass through the Constant Systems Cell Disruptor (Warwick, UK) at  $20.3 \text{ kpsi.}$  The disrupted cells were centrifuged at  $16\,000 \text{ g}$  in a benchtop centrifuge (Denville Scientific 260D) for  $5 \text{ min}$ , and the supernatant was assayed for protein concentration using the BCA Protein Assay kit from Pierce (Rockford, IL). The whole-cell activity was calculated by normalizing the initial rate of substrate conversion or product formation to the protein concentration.

### Identification of products

*Escherichia coli* JM109 cells with WT or mutant plasmid were grown, induced, washed and resuspended in modified M9 medium, as described for the whole-cell activity assay. Substrate was added to a final concentration of  $1 \text{ mM}$  to  $40 \text{ mL}$  of the resuspended cells, and the resting cell culture

was incubated at 30 °C for 3 h in a shaking incubator at 250 r.p.m. The culture was then centrifuged at 6000 *g* for 10 min (Beckman J2-21M centrifuge with a JA14 rotor), and the supernatant was extracted with ethyl acetate. The ethyl acetate was then evaporated with a rotary evaporator under vacuum at 40 °C, and the residue was dissolved in 5 mL of methanol. The sample was then analyzed by LC-MS with an Agilent series 1100 HPLC (Agilent Technologies, Palo Alto, CA) coupled to an Applied Biosystems 4000 Q-Trap mass spectrometer. Separation was achieved with the 250 × 4.60 mm Synergi 4 μ Polar-RP 80 A column from Phenomenex. Isocratic methods with a flow rate of 0.4 mL·min<sup>-1</sup> were used for all analyses. The aniline conversion product was analyzed using 60% 20 mM ammonium acetate (pH 5.4) and 40% acetonitrile as mobile phase. The 2IPA conversion product was analyzed using 50% 20 mM ammonium acetate (pH 5.4) and 50% acetonitrile as mobile phase. The 24DMA conversion product was analyzed using 40% 20 mM ammonium acetate (pH 5.4) and 60% acetonitrile as mobile phase. Negative ESI mode with declustering potential and collision energies of -70 eV and -20 eV, respectively, was employed.

For <sup>1</sup>H-NMR analysis of the product of 24DMA conversion, the above assay was repeated using 200 mL of resuspended cells. After the extraction and evaporation of ethyl acetate, the sample was dissolved in a mixture of 95% chloroform and 5% methanol. The 24DMA dihydroxylation product was then purified using silica gel chromatography, with a mixture of 95% chloroform and 5% methanol as the mobile phase. The fraction containing the product was collected and dried with a rotary evaporator under vacuum at 40 °C. The sample was dissolved in CDCl<sub>3</sub> and analyzed by 500 MHz <sup>1</sup>H-NMR (Bruker AMX500, Billerica, MA) using tetramethylsilane as internal standard.

## Acknowledgements

This work was supported by the US Department of Energy and the A\*STAR program in Singapore. We would like to thank M. Takeo from the Department of Applied Chemistry, Himeiji Institute of Technology, Hyogo, Japan, for providing us with the pAS91 and pAS93 plasmids, and Z. Jie from the Tropical Marine Science Institute, National University of Singapore, Singapore, for his kind assistance with the LC-MS analyses.

## References

1 Grayson M, Eckroth D, Mark HFF, Othmer D, Overberger CG & Seaborg GT (1984) *Kirk-Othmer Encyclopedia of Chemical Technology*, Vol. 2, 3rd edn, pp. 309–375. John Wiley & Sons, New York, NY.

- Radomski JL (1979) The primary aromatic amines: their biological properties and structure–activity relationships. *Annu Rev Pharmacol Toxicol* **19**, 129–157.
- Rai HS, Bhattacharyya MS, Singh J, Bansal TK, Vats P & Banerjee UC (2005) Removal of dyes from the effluent of textile and dyestuff manufacturing industry: a review of emerging techniques with reference to biological treatment. *Crit Rev Environ Sci Technol* **35**, 219–238.
- Bomhard EM & Herbold BA (2005) Genotoxic activities of aniline and its metabolites and their relationship to the carcinogenicity of aniline in the spleen of rats. *Crit Rev Toxicol* **35**, 783–835.
- Przybojewska B (1999) Assessment of aniline derivatives-induced DNA damage in the liver cells of B6C3F1 mice using the alkaline single cell gel electrophoresis ('comet') assay. *Cancer Lett* **147**, 1–4.
- Shardonofsky S & Krishnan K (1997) Characterization of methemoglobinemia induced by 3,5-xylydine in rats. *J Toxicol Environ Health* **50**, 595–604.
- Nohmi T, Miyata R, Yoshikawa K, Nakadate M & Ishidate M Jr (1983) Metabolic activation of 2,4-xylydine and its mutagenic metabolite. *Biochem Pharmacol* **32**, 735–738.
- Weisburger EK, Russfield AB, Homburger F, Weisburger JH, Boger E, Dongen CGV & Chu KC (1978) Testing of twenty-one environmental aromatic amines or derivatives for long-term toxicity or carcinogenicity. *J Environ Pathol Toxicol* **2**, 325–356.
- Markowitz SB & Levin K (2004) Continued epidemic of bladder cancer in workers exposed to ortho-toluidine in a chemical factory. *J Occup Environ Med* **46**, 154–160.
- Lyons CD, Katz S & Bartha R (1984) Mechanisms and pathways of aniline elimination from aquatic environments. *Appl Environ Microbiol* **48**, 491–496.
- Bugg TDH & Winfield CJ (1998) Enzymatic cleavage of aromatic rings: mechanistic aspects of the catechol dioxygenases and later enzymes of bacterial oxidative cleavage pathways. *Nat Prod Rep* **15**, 513–530.
- Takeo M, Fujii T & Maeda Y (1998a) Sequence analysis of the genes encoding a multicomponent dioxygenase involved in oxidation of aniline and o-toluidine in *Acinetobacter* sp. strain YAA. *J Ferment Bioeng* **85**, 17–24.
- Takeo M, Fujii T, Takenaka K & Maeda Y (1998b) Cloning and sequencing of a gene cluster for the meta-cleavage pathway of aniline degradation in *Acinetobacter* sp. strain YAA. *J Ferment Bioeng* **85**, 514–517.
- Fukumori F & Saint CP (1997) Nucleotide sequences and regulational analysis of genes involved in conversion of aniline to catechol in *Pseudomonas putida* UCC22 (pTDN1). *J Bacteriol* **179**, 399–408.
- Tan HM & Cheong CM (1994) Substitution of the ISP alpha subunit of biphenyl dioxygenase from *Pseudomonas* results in a modification of the enzyme activity. *Biochem Biophys Res Commun* **204**, 912–917.

- 16 Parales RE, Emig MD, Lynch NA & Gibson DT (1998) Substrate specificities of hybrid naphthalene and 2,4-dinitrotoluene dioxygenase enzyme systems. *J Bacteriol* **180**, 2337–2344.
- 17 Parales JV, Parales RE, Resnick SM & Gibson DT (1998) Enzyme specificity of 2-nitrotoluene 2,3-dioxygenase from *Pseudomonas* sp. strain JS42 is determined by the C-terminal region of the alpha subunit of the oxygenase component. *J Bacteriol* **180**, 1194–1199.
- 18 Kumamaru T, Suenaga H, Mitsuoka M, Watanabe T & Furukawa K (1998) Enhanced degradation of polychlorinated biphenyls by directed evolution of biphenyl dioxygenase. *Nat Biotechnol* **16**, 663–666.
- 19 Parales RE, Resnick SM, Yu CL, Boyd DR, Sharma ND & Gibson DT (2000) Regioselectivity and enantioselectivity of naphthalene dioxygenase during arene cis-dihydroxylation: control by phenylalanine 352 in the alpha subunit. *J Bacteriol* **182**, 5495–5504.
- 20 Parales RE, Lee K, Resnick SM, Jiang H, Lessner DJ & Gibson DT (2000) Substrate specificity of naphthalene dioxygenase: effect of specific amino acids at the active site of the enzyme. *J Bacteriol* **182**, 1641–1649.
- 21 Barriault D & Sylvestre M (2004) Evolution of the biphenyl dioxygenase BphA from *Burkholderia xenovorans* LB400 by random mutagenesis of multiple sites in region III. *J Biol Chem* **279**, 47480–47488.
- 22 Barriault D, Plante MM & Sylvestre M (2002) Family shuffling of a targeted *bphA* region to engineer biphenyl dioxygenase. *J Bacteriol* **184**, 3794–3800.
- 23 Leungsakul T, Keenan BG, Yin H, Smets BF & Wood TK (2005) Saturation mutagenesis of 2,4-DNT dioxygenase of *Burkholderia* sp. strain DNT for enhanced dinitrotoluene degradation. *Biotechnol Bioeng* **92**, 416–426.
- 24 Keenan BG, Leungsakul T, Smets BF & Wood TK (2004) Saturation mutagenesis of *Burkholderia cepacia* R34 2,4-dinitrotoluene dioxygenase at DntAc valine 350 for synthesizing nitrohydroquinone, methylhydroquinone, and methoxyhydroquinone. *Appl Environ Microbiol* **70**, 3222–3231.
- 25 Keenan BG, Leungsakul T, Smets BF, Mori MA, Henderson DE & Wood TK (2005) Protein engineering of the archetypal nitroarene dioxygenase of *Ralstonia* sp. strain U2 for activity on aminonitrotoluenes and dinitrotoluenes through alpha-subunit residues leucine 225, phenylalanine 350, and glycine 407. *J Bacteriol* **187**, 3302–3310.
- 26 Sakamoto T, Joern JM, Arisawa A & Arnold FH (2001) Laboratory evolution of toluene dioxygenase to accept 4-picoline as a substrate. *Appl Environ Microbiol* **67**, 3882–3887.
- 27 Fujii T, Takeo M & Maeda Y (1997) Plasmid-encoded genes specifying aniline oxidation from *Acinetobacter* sp strain YAA. *Microbiology* **143**, 93–99.
- 28 Kauppi B, Lee K, Carredano E, Parales RE, Gibson DT, Eklund H & Ramaswamy S (1998) Structure of an aromatic-ring-hydroxylating dioxygenase-naphthalene 1,2-dioxygenase. *Structure* **6**, 571–586.
- 29 Furusawa Y, Nagarajan V, Tanokura M, Masai E, Fukuda M & Senda T (2004) Crystal structure of the terminal oxygenase component of biphenyl dioxygenase derived from *Rhodococcus* sp. strain RHA1. *J Mol Biol* **342**, 1041–1052.
- 30 Dong X, Fushinobu S, Fukuda E, Terada T, Nakamura S, Shimizu K, Nojiri H, Omori T, Shoun H & Wakagi T (2005) Crystal structure of the terminal oxygenase component of cumene dioxygenase from *Pseudomonas fluorescens* IP01. *J Bacteriol* **187**, 2483–2490.
- 31 Meyer A, Schmid A, Held M, Westphal AH, Rothlisberger M, Kohler HP, van Berkel WJ & Witholt B (2002) Changing the substrate reactivity of 2-hydroxybiphenyl 3-monooxygenase from *Pseudomonas azelaica* HBP1 by directed evolution. *J Biol Chem* **277**, 5575–5582.
- 32 Kunz DA & Chapman PJ (1981) Catabolism of pseudocumene and 3-ethyltoluene by *Pseudomonas putida* (arvilla) mt-2: evidence for new functions of the TOL (pWWO) plasmid. *J Bacteriol* **146**, 179–191.
- 33 Wackett LP (2002) Mechanism and applications of Rieske non-heme iron dioxygenases. *Enzyme Microb Tech* **31**, 577–587.
- 34 Beil S, Mason JR, Timmis KN & Pieper DH (1998) Identification of chlorobenzene dioxygenase sequence elements involved in dechlorination of 1,2,4,5-tetrachlorobenzene. *J Bacteriol* **180**, 5520–5528.
- 35 Karlsson A, Parales JV, Parales RE, Gibson DT, Eklund H & Ramaswamy S (2003) Crystal structure of naphthalene dioxygenase: side-on binding of dioxygen to iron. *Science* **299**, 1039–1042.
- 36 Parales RE, Parales JV & Gibson DT (1999) Aspartate 205 in the catalytic domain of naphthalene dioxygenase is essential for activity. *J Bacteriol* **181**, 1831–1837.
- 37 Rui L, Kwon YM, Fishman A, Reardon KF & Wood TK (2004) Saturation mutagenesis of toluene orthomonooxygenase of *Burkholderia cepacia* G4 for enhanced 1-naphthol synthesis and chloroform degradation. *Appl Environ Microbiol* **70**, 3246–3252.
- 38 Ju KS & Parales RE (2006) Control of substrate specificity by active-site residues in nitrobenzene dioxygenase. *Appl Environ Microbiol* **72**, 1817–1824.
- 39 Pollmann K, Wray V, Hecht HJ & Pieper DH (2003) Rational engineering of the regioselectivity of TecA tetrachlorobenzene dioxygenase for the transformation of chlorinated toluenes. *Microbiology* **149**, 903–913.
- 40 Fuenmayor SL, Wild M, Boyes AL & Williams PA (1998) A gene cluster encoding steps in conversion of naphthalene to gentisate in *Pseudomonas* sp. strain U2. *J Bacteriol* **180**, 2522–2530.
- 41 Zylstra GJ & Gibson DT (1989) Toluene degradation by *Pseudomonas putida* F1. Nucleotide sequence of the

- todC1C2BADE* genes and their expression in *Escherichia coli*. *J Biol Chem* **264**, 14940–14946.
- 42 Erickson BD & Mondello FJ (1992) Nucleotide sequencing and transcriptional mapping of the genes encoding biphenyl dioxygenase, a multicomponent polychlorinated-biphenyl-degrading enzyme in *Pseudomonas* strain LB400. *J Bacteriol* **174**, 2903–2912.
- 43 Taira K, Hirose J, Hayashida S & Furukawa K (1992) Analysis of *bph* operon from the polychlorinated biphenyl-degrading strain of *Pseudomonas pseudoalcaligenes* KF707. *J Biol Chem* **267**, 4844–4853.
- 44 Yamashita MM, Almasy RJ, Janson CA, Cascio D & Eisenberg D (1989) Refined atomic model of glutamine synthetase at 3.5 Å resolution. *J Biol Chem* **264**, 17681–17690.
- 45 Tesmer JJ, Klem TJ, Deras ML, Davisson VJ & Smith JL (1996) The crystal structure of GMP synthetase reveals a novel catalytic triad and is a structural paradigm for two enzyme families. *Nat Struct Biol* **3**, 74–86.
- 46 Thomas MR (1994) Simple, effective cleanup of DNA ligation reactions prior to electro-transformation of *E. coli*. *Biotechniques* **16**, 988–990.
- 47 Sambrook J, Fritsch EF & Maniatis T (1989) *Molecular Cloning: a Laboratory Manual*. Cold Spring Harbor Laboratory Press, Cold Spring Harbor, NY.

## Supplementary material

The following supplementary material is available online:

**Table S1.** Primers used in the cloning of the *atdA1–A5* gene. Underlined bases represent the respective restriction sites.

**Table S2.** Primers used in saturation mutagenesis. Underlined bases represent the randomized codon, where N = G, C, A or T, and S = G or C.

**Fig. S1.** SDS/PAGE of the soluble fraction (A) and total fraction (B) of *E. coli* JM109 expressing the WT, V205A mutant and I248L mutant AtdA.

This material is available as part of the online article from <http://www.blackwell-synergy.com>

Please note: Blackwell Publishing is not responsible for the content or functionality of any supplementary materials supplied by the authors. Any queries (other than missing material) should be directed to the corresponding author for the article.